Tellus (2007), 59, 673–684
Printed in Singapore. All rights reserved

TELLUS

Methanol and acetaldehyde fluxes over ryegrass

By THOMAS CUSTER[†] and GUNNAR SCHADE[*,‡], *Institut für Umweltphysik (IUP), Universität Bremen, 28359 Bremen, Germany*

(Manuscript received 28 June 2006; in final form 14 May 2007)

ABSTRACT

Oxygenated volatile organic compounds (OVOCs) play an active role in tropospheric chemistry but our knowledge concerning their release and ultimate fate is limited. However, the recent introduction of Proton Transfer Reaction Mass Spectrometry (PTRMS) has improved our capability to make direct field observations of OVOC mixing ratios and fluxes. We used PTRMS in an eddy covariance setup to measure selected OVOC exchange rates above a well-characterized agricultural plot in Northern Germany. In fall 2003, mixing ratios of methanol and acetaldehyde 2 m above the field ranged from 1 to 10 and 0.4 to 2.1 ppb, respectively, well correlated with one another. Fluxes of both gases were followed for growing Italian ryegrass (*Lolium multiflorum*) over a significant portion of its life cycle. Diurnally fluctuating emissions of methanol and very small acetaldehyde fluxes were observed up to the cutting and removal of the grass. Methanol emissions were exponentially related to ambient temperatures and appeared to be higher during the grass' rapid leaf area expansion and after a rain event. Acetaldehyde exchanges averaged over the whole period indicated very slow deposition. Our measurements confirm previous, similar results, as well as presumptions that grasses are comparatively low methanol emitters compared to non-grass species.

1. Introduction

Many volatile organic compounds (VOCs) have been investigated by the atmospheric community related, among other processes, to tropospheric O_3 production and their roles as aerosol precursors (Chameides et al., 1988, 1992; McKeen et al., 1991; Andreae and Crutzen, 1997; Sillman, 1999). The abundant hydrocarbon isoprene (2-methyl-1,3-butadiene, C_5H_8) and related plant terpenoids, in particular monoterpenes ($C_{10}H_{16}$) have long been recognized as significant participants in atmospheric chemistry. As knowledge concerning isoprene and monoterpenes has rapidly expanded, it has also become clear that a diverse mixture of oxygenated VOCs (OVOCs) can at times constitute a significant or even dominant portion of total VOC loading in the troposphere and that these compounds can impact tropospheric chemistry at different scales (Arey et al. 1991; Winer et al., 1992; König et al. 1995; Fukui and Doskey, 1998; Kirstine et al. 1998; Riemer et al., 1998; Fall et al., 1999; Singh et al., 2000; Karl et al., 2001b; Schade and Goldstein, 2001).

A wide range of chemicals fall under the OVOC rubric, the majority of which are thought to be biogenic rather than anthropogenic in origin (Guenther et al., 1995) and may be primary emissions or secondary oxidation products of directly emitted species. In rural environments, vegetation is thought to be the most important direct source of certain OVOCs. Documented OVOC releases from live green, wounded, senescing or decaying plant material, include species such as methanol, ethanol, acetaldehyde, acetone, 2-butanone, formic and acetic acids, hexenals and hexenols, just to name a few (Kesselmeier et al., 1997; de Gouw et al., 1999; Warneke et al., 1999; Karl et al., 2001a, 2003; Custer et al., 2003). Although our understanding of the plant biochemical origins of the most abundant of these OVOCs is gradually improving (Sharkey, 1996; Fall 1999, 2003; Kesselmeier and Staudt, 1999; Kesselmeier, 2001; Schnitzler et al., 2002; Custer et al., 2003), it remains challenging to move from this knowledge to an accurate prediction of primary OVOC emissions from plants to the troposphere (Harley et al., 2004). This is due to the great diversity of plants, the complexity of plant metabolism, and uncertainties in how various environmental factors affect both of these.

Direct measurements of OVOC fluxes provide a picture of OVOC cycling that encompasses the complex interactions between all contributors in a localized area. By examining a diverse set of flux measurements spanning representative ecosystems around the globe, a better understanding of proposed

*Corresponding author.
e-mail: schade@ariel.met.tamu.edu
[†]Present address: Max Planck Institut für Chemie, 55128 Mainz, Germany.
[‡]Present address: Department of Atmospheric Sciences, Texas A & M University, College Station, TX 77843, USA.
DOI: 10.1111/j.1600-0889.2007.00294.x

budgets and chemistry can be obtained. Crop and grasslands cover a significant area of the earth and, although they are negligible isoprene emitters, they may be a significant source of a number of other OVOCs such as methanol, acetaldehyde, or acetone (Fukui and Doskey, 1998; de Gouw et al., 2000; Karl et al., 2001a, b; Warneke et al., 2002; Karl et al., 2005b). Croplands can also be a particularly convenient location for micrometeorological flux measurements, often presenting extended, homogeneous flux footprints with a well-defined selection of plants and soils.

Here, we report on field measurements of mixing ratios and eddy covariance fluxes of methanol and acetaldehyde above a farm field growing ryegrass as an intermediate crop. Methanol and acetaldehyde have attracted interest due to their roles in tropospheric HO_x chemistry. Methanol is often the second most abundant VOC after methane in the troposphere. Due to its comparatively long lifetime of approximately 1 week, it can serve as a significant source of HO_x in the free and upper troposphere (Tie et al., 2004). Its budget has been discussed in numerous recent works (Singh et al., 2000, 2004; Heikes et al., 2002; Galbally and Kirstine, 2002; Jacob et al., 2005). Green plant emissions probably comprise approximately two-thirds of the methanol budget, and are thought to arise from demethylation of pectin during plant cell wall expansion (Fall and Benson, 1996; Galbally and Kirstine, 2002). Several recent field works have confirmed significant methanol fluxes from green plants (Fukui and Doskey, 1998; Kirstine et al., 1998; Baker et al., 2001; Schade and Goldstein, 2001; Warneke et al., 2002; Karl et al., 2003, 2004) and soil (Schade and Goldstein, 2001; Schade and Custer, 2004; Rinnan et al., 2005), but a number of emission characteristics remain unexplored. Other important sources include biomass burning (Holzinger et al., 1999; Goode et al., 1999; Yokelson et al., 1999), and photochemical production from methane under very low NO_x conditions. The major sink of methanol is through reaction with hydroxyl radicals, and there are presumably minor contributions from wet and dry deposition (Jacob et al., 2005).

Acetaldehyde is a much shorter lived species in the atmosphere compared to methanol. Its lifetime is on the order of 1 d as determined by both OH radical reactions and photolysis. A rough global budget has recently been published by Singh et al. (2004) suggesting a global source of 200 ± 85 Tg yr^{-1} dominated by oceanic emissions. Aside from this source, acetaldehyde is a secondary product of the oxidation of alkanes and 2-alkenes of both anthropogenic and biogenic origins, is a directly emitted product of biomass burning (Holzinger et al., 1999) and cut and decaying vegetation (de Gouw et al., 1999; Warneke et al., 2002), and can be released directly by green plants (Kreuzwieser et al., 1999, 2000; Karl et al., 2003, 2005a; Graus et al., 2004). Acetaldehyde, like methanol, is ubiquitous in the troposphere a fact which is likely related to its diverse sources (Singh et al., 2004).

2. Experimental

2.1. Field site

Measurement equipment was located near the centre of a 20 ha field of the 181 ha experimental farm of the Bundesforschungsanstalt für Landwirtschaft (FAL) that lies to the NW of Braunschweig (population: 240 000, 1250 km^{-2} on 190 km^2), Germany (52° 17′ 50N, 10° 27′E, 81 m a.s.l.). The experimental farm field is organized for intensive cereal and fodder production. Crops rotate between barley, winter wheat, sugar beet and ryegrass. Measurements reported here extended over much of the lifetime of a crop of Italian ryegrass (*Lolium multiflorum*) seeded in September of 2003. Soil, nutrients, and pesticides in the field are managed according to current farm practices and the field is irrigated as necessary. The soil is a loamy sand (cambisol) with an average pH of 6.5, organic matter content of 1.4 $\pm$ 0.1% with soil water content ranging between 22 and 5%. The field extends approximately 200 m both E and W from the micrometeorological instrumentation and is bounded by a dirt road on both sides, followed by additional fields extending a few hundred metres more. For various portions of the measurement period, adjacent fields were sown with maize or clover whose development did not necessarily track that of the crop immediately under study. To the north of the measurement equipment, the field is bounded by a row of trees and bushes ~200 m distant and on the south by another dirt road ~350 m distant. A number of animal sheds, housing mainly cows, lie ~600 m distant to the SW. A row of buildings and a meteorological station of the Deutsche Wetterdienst (DWD, German Weather Service) Agrometeorological Research branch stand at a distance of ~650 m directly south near the edge of a small, forested area. The dominant trees in this suburban and agricultural region are European beech and common oak, with lesser numbers of Norway spruce, hornbeam, and larch. The nearest paved road lies to the *E* of the experimental fields ~600 m distant and carries ~41 cars min^{-1} during daytime hours.

2.2. Instrumental set-up

The eddy covariance technique relies on colocated, simultaneous, and fast measurements of vertical wind velocity and OVOC mixing ratios to determine OVOC fluxes. A schematic of the experimental set-up is given in Fig. 1. A Solent R3 sonic anemometer (Gill Instruments, UK) mounted on a 2 m pole was used to measure 3-D wind velocities and virtual temperature at the centre of the farm field. This anemometer was originally installed by the FAL in 1999 and is operated using Edibox data acquisition and EdiSol software (Moncrieff et al., 1997). For fast monitoring of OVOC mixing ratios, a proton-transfer-reaction mass spectrometer (PTR-MS, Ionicon Analytik GmbH, Innsbruck, Austria) was installed in a wooden shed that was located ~12 m to the E of the anemometer so as not to interfere with the turbulence mea-

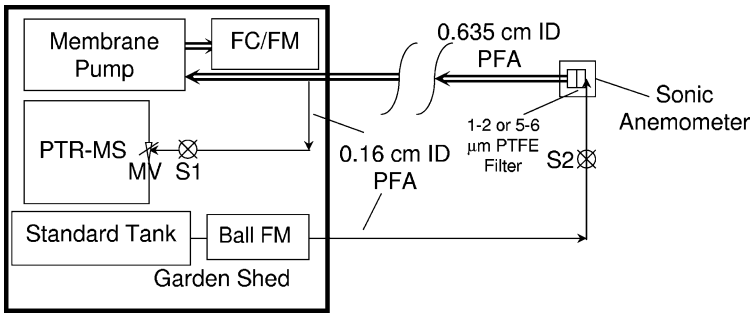

Fig. 1. Schematic of the FAL field set-up (not to scale).

surements under the typical, westerly wind directions. The shed, supplied with line power that had been previously run to the centre of the field, was insulated and air-conditioned to provide adequate conditions for an extended, seasonal deployment of the mass spectrometer.

For routine measurements, a membrane air sampling pump (Rietschle Thomas model LM22) was used to pull air through approximately 15 m of 0.635 cm ID Teflon PFA tubing that ran from the head of the anemometer to the wooden shed where it was subsampled into the mass spectrometer through ∼0.5 m of 1.6 mm ID Teflon PFA tubing, a Teflon PTFE shut-off valve, and ∼0.5 m 1 mm ID of heated Silcosteel tubing inside the PTR-MS. The inlet of the transfer tubing was equipped with either a 1–2 or 5–6 μm Teflon PTFE filter in a PFA filter holder positioned under the anemometer in order to remove particulate matter from the air stream. These filters were replaced on a weekly basis. Flow through the sampling line was regulated to ∼9 L min^{-1} using a ball flow meter equipped with a metering valve attached at the exhaust of the membrane pump. Air from this main sample line was subsampled by the PTR-MS at flow rates of ∼100 cm^3 min^{-1}. Both the Silcosteel tubing and the instrument's drift tube were heated to 40 °C. A pressure controller regulates the pressure immediately prior to the entrance to the drift tube, helping to maintain a steady ∼15 STP cm^3 min^{-1} flow of sample air into the drift region regardless of changes in ambient pressure. The overall subsampling flow rate was not monitored and changed with every exchange of the mass spectrometer ion source which occurred on a monthly basis.

An additional 1.6 mm ID line was run from the shed to a Teflon PTFE solenoid shut-off valve (Parker Hannifin, USA) in a water-tight container near the head of the anemometer and was ultimately connected via a TEE to the head of the sampling line. This line delivered gas from a standard tank containing ppm concentrations of methanol in N_2 (Air Liquide, Germany) to the main sampling line for periodic calibrations. The calibration valve was controlled by the PTR-MS computer that started or stopped standard addition at prescribed intervals. Flows were regulated using a 1–20 cm^3 min^{-1} ball flow metre.

Signals for u, v and w wind velocities and speed-of-sound were sent via the Solent R3 PCIA box analogue outputs to the analogue input collection board of the PTR-MS instrument. Both ion signal intensities and data from the anemometer were then stored in parallel on the laptop PC of the PTR-MS. Two data collection routines and one calibration routine were used during the course of experiments. In the data collection routines, which alternated every half hour, the signal from ions at either m/z 33 or m/z 45 were monitored for 0.2 s, followed immediately by collection of the u, v, w and speed-of-sound output of the anemometer. The result was a data set with a measurement frequency very near 4 Hz and spanning just less than 30 min (7110 total cycles per half hour) that was used for flux calculations. An allowance of ∼5 s was left at the end of each 30 min period to prevent data loss otherwise experienced over extended, unattended measurement. Hence, in 1 h fluxes for two different compounds (methanol and acetaldehyde) were obtained using this method. Interleaved with the data collection routines was a 30-min calibration routine executed at 8-h intervals. It incorporated measurements of a much broader selection of ions but no signals from the anemometer. These ion signals were monitored for a total of 194 cycles accounting for ∼21 out of 30 min. The first 40 of these cycles were devoted to measurement of ambient air with no change in air sampling procedure. At cycle 40, the solenoid valve controlling the addition of standard gas to the main transfer line was opened, and upon the last cycle the valve was once again closed and mass scans (ranging from m/z 20 to 150) were executed for the remainder of the 30-min time period while the calibration gas was flushed from the line by ambient air.

2.3. Data analysis

All data were analysed using R-language open source software (R Development Core Team, 2005). Wind velocities were first treated by converting speed-of-sound to virtual temperature and by removing spikes according to Højstrup (1993), then rotating into streamline coordinates (Kaimal and Finnigan, 1994). A Gaussian high pass filter having a width of 5 data points (∼1.25 s for 4 Hz data) was then applied to reduce white noise in the signals. Identical de-spiking and filtering was performed on mixing ratios computed from PTR-MS data. The $w'\mu'$ covariance, where μ represents the mixing ratio, was then calculated and converted from units of ppbv m^{-2} h^{-1} to units of mg C m^{-2} h^{-1}

using an assumed atmospheric pressure of 100 kPa and virtual temperature. In addition to OVOC fluxes, friction velocity, u^*, sensible heat flux, H, and Monin-Obuhkov length, L, were calculated using a default specific humidity of 6.4 g kg^{-1}.

In the PTR-MS, sampled VOCs having a proton affinity greater than that of water are ionised through proton-transfer-reactions with abundant 'parent' H_3O^+ ions inside a high-pressure (~2 mbar) reaction drift tube. Both parent and protonated product ions are then sampled into the vacuum of a quadrupole mass spectrometer for separation and detection. Product ion signals at m/z 33 from the PTR-MS were converted to mixing ratios of methanol, μ_{33}, using

$$\mu_{33} = (S_{33} - S_{32} \times 0.00076)\frac{10^6}{(S_{21} \times 500)}\frac{1}{\mathrm{NCF}_{33}}, \qquad (1).$$

where μ_{33} is the calculated mixing ratio (in ppb), S_{33} and S_{21} are ion count rates (cps) for the protonated methanol product ion and parent H_3O^+ ion, respectively, and NCF_{33} is a normalized calibration factor (ncps ppb^{-1}). The subtracted term, $S_{32} \times 0.00076$, is the contribution of the $^{16}O^{17}O^+$ isotope to the signal at m/z 33. Measured values at m/z 25, a signal generally used as a proxy for detector noise and often very near zero in mass spectrometers as well as for these data, were also subtracted from the signals S_{33} and S_{21}. These corrections represent only a part of the total background and were subtracted in lieu of more complete data as subsequently described. The product ion signal intensity (term 1 of eq. 1) was normalized to 10^6 cps of H_3O^+ as has been done elsewhere (Warneke et al., 2002, 2003; de Gouw et al., 2003a), mainly to facilitate intercomparison between these measurements and those made on similar instruments whose parent ion count rate and other operating parameters may not be identical. Normalized calibration factors were obtained through addition of a methanol standard gas to the sampling line at regular intervals throughout the experiment. The dilution of the standard was calculated by multiplying the known concentration of the tank by the ratio of the standard gas flow rate to the flow rate of the main sampling line. No similar standard was available for acetaldehyde. Figure 2 shows the development of the methanol calibration factor and subtracted portions of background over the period of measurements discussed here. Abrupt changes such as on days 260, 265, 269 and 274 were due to changes in instrument settings such as the water flow into the ion source and the secondary electron multiplier detector voltage. Further structure was likely due to drifting flow rates and variations in ambient air mixing ratios which may have obscured measured changes in signal. Overall precision of the calibration factors, based on the standard deviation of measured signals and conservative error estimates in flow rates of 1 mL min^{-1} for the calibration gas and 500 cm^3 s^{-1} for the sampling line flow, were between 20 and 30%. These values reflect measurements at mixing ratios in the range observed in this work and will also be representative of the overall precision of mixing ratios.

As a standard for acetaldehyde was not available, mixing ratios were determined directly using eq. 2 (de Gouw et al., 2003a)

$$\mu_i = -1.4 \times 10^{-18}\frac{T^2 V}{k d^2 P^2}\ln\left(\frac{\frac{(S_{21}\times 500)}{TF_{21}}}{\frac{(S_{21}\times 500)}{TF_{21}} + \frac{(S_i)}{TF_i}}\right), \qquad (2).$$

where T is the temperature of the reaction drift tube in Kelvin, V is the voltage applied across the drift tube (500 V), k is the rate coefficient for reaction between H_3O^+ and the VOC of interest (cm^3 molec^{-1} s^{-1}), d is the length of the drift tube (9.5 cm), P is the pressure in the drift tube (2.1 mbar), $S_{21} \times 500$ is the count rate used as a proxy for measurement of the $H_3{}^{16}O^+$ parent ion, and TF_{21} and TF_i are instrument specific transmission factors for m/z 21 (0.5) and the m/z of interest, respectively. Transmission factors provided by the instrument manufacturer were used for these calculations (0.7 for m/z 33 and 0.9 for m/z 45) although

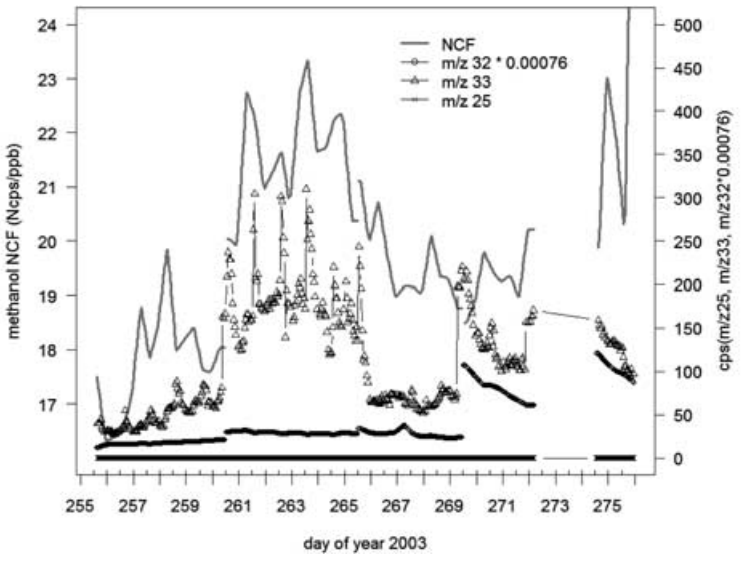

Fig. 2. Variation of the normalized calibration factor (NCF) and ambient signal for m/z 33, subtracted isotopic $O_2{}^+$ background (from measurements at m/z 32), and instrument noise at m/z 25 during the relevant data period in September 2003.

field-operating conditions different from those of the factory determination as well as the condition of the secondary electron multiplier may cause some error (e.g. Steinbacher et al., 2004). Normalized calibration factors of 20 and 34, calculated using an H_3O^+ reduced mobility of 2.8 $cm^2\ V^{-1}\ s^{-1}$, rate coefficients for reactions between H_3O^+ and methanol/acetaldehyde of 2.6 and $3.6 \times 10^{-9}\ cm^3\ molec^{-1}\ s^{-1}$, and the above listed transmission factors, drift tube pressure, drift tube length, and drift field, were applied in mixing ratio calculations of methanol and acetaldehyde where no experimentally determined values were available. Good agreement between experimentally determined and calculated NCF values for methanol suggest that factory transmission factors were adequate, however no independent determination was performed successfully.

To completely account for background signal at each channel of the PT-RMS, a combination of measurements of zero air (to determine contributions from instrument surfaces, ion source, flow/drift tube and detector) and hyphenation with gas chromatography (to determine chemical cross talk between channels due to formation of isobaric or identical ions of differing origin) are necessary. As neither a catalytic converter nor a gas chromatograph were available for these experiments, and as performance of such measurements would severely inhibit our ability to measure at frequencies required for eddy covariance measurements, background determination in this manner was impossible. Partial background contributions as in the case of the $^{16}O^{17}O^+$ contribution to the methanol signal at m/z 33 or detector background (taken from m/z 25), both shown in Fig. 2, were obtained from the calibration measurements spaced at 8-h intervals and then linearly interpolated and applied to the higher frequency measurements.

The potential overestimate of the mixing ratio accrued by such partial background correction is estimated to have typically been 0.5 ppb for methanol and less than 0.5 ppb for acetaldehyde based on measurements during the following year using a catalytic converter. Additional error from the use of eq. 2 or unaccounted-for chemical cross-talk should be low. From our own observations and the work of others, neither protonated methanol nor acetaldehyde product ions undergo significant fragmentation. Interferences with other compounds have also been previously investigated for these compounds using gas chromatographic separation of air samples followed by detection using the PTR-MS (de Gouw et al., 2003a; Warnecke et al., 2003). In representative rural and urban air samples, methanol was deemed free of interference from other compounds provided background was accounted for. Acetaldehyde exhibited some dependence on the CO_2 mixing ratio, possibly due to endothermic HCO_2^+ formation. While the effect was implied as being minor overall, its contribution to our own data cannot be evaluated without a complementary data set for CO_2 and more in depth study of the hypothetical process suggested for formation of HCO_2^+. Acetaldehyde is also known to be produced in Teflon lines in the presence of high amounts of ozone (Northway et al., 2004). Again, without complementary ozone data such interferences cannot be ruled out or corrected for, although it should be noted that these interferences are small and likely play a minor role in the boundary layer where our own measurements took place (Goldan et al., 2004).

Based on this discussion, all presented mixing ratios have to be interpreted as upper limits. However, overestimation of mixing ratios will not affect flux values, which are calculated based on covariance of deviations from a 30 min average value. It is assumed that fast fluctuations are detectable within the precision of the measurement, generally on the order of 30% similar to what was observed for our measurements of normalized calibration factors, and can reliably be used for such calculations.

Other aspects of the experimental set-up may affect the accuracy of a flux determination. Transport of OVOCs from the head of the anemometer to the PTR-MS instrument for analysis creates a lag-time between the wind velocity and the ion signal measurement and has the potential to introduce line artefacts (Karl et al., 2002, and references therein). The tubing lag-time can be assessed in a number of ways, and we have previously used both transport volume and flow calculations, phase spectrum analysis, and maximum w–μ correlations to calculate the lag-time in our field set-up (Schade and Custer, 2004). To arrive at the best lag-time estimate for the data presented here, the lag-time was determined through the latter method by systematically shifting the vertical wind velocity vector with respect to the mixing ratio vector in time. At each point, the flux and correlation coefficient were calculated. When fluxes were significant, a distinct maximum or minimum in the flux (or correlation coefficient) could be observed in a plot of lag time versus flux (Fig. 3). When a significant flux was observed, the lag time of its maximum value was chosen and these values are reported. When no significant flux existed or there was no clear maximum or minimum, the choice of flux was determined using lag times observed for adjacent collection periods when a flux was apparent.

For the above listed flow and tubing conditions, Reynolds numbers around 2000 were calculated, indicating only slightly turbulent conditions during line transport. Whether this caused a significant line-loss of eddies contributing to the calculated flux under the local turbulence conditions was previously assessed by comparing $w'T'$ to $w'\mu'$ cospectra in the inertial subrange (Schade and Custer, 2004). For the data presented here, analysing medium to high fluxes of methanol in a similar way showed that there was no trend towards a steeper slope in the inertial subrange of the $w'\mu'$ compared to the $w'T'$ cospectrum. Therefore, no corrections or adjustments were made to the calculated fluxes in this work.

3. Results and discussion

Figure 4 shows the measured mixing ratios of methanol and acetaldehyde along with air temperature and precipitation at the nearby DWD weather station. Blank areas represent times when

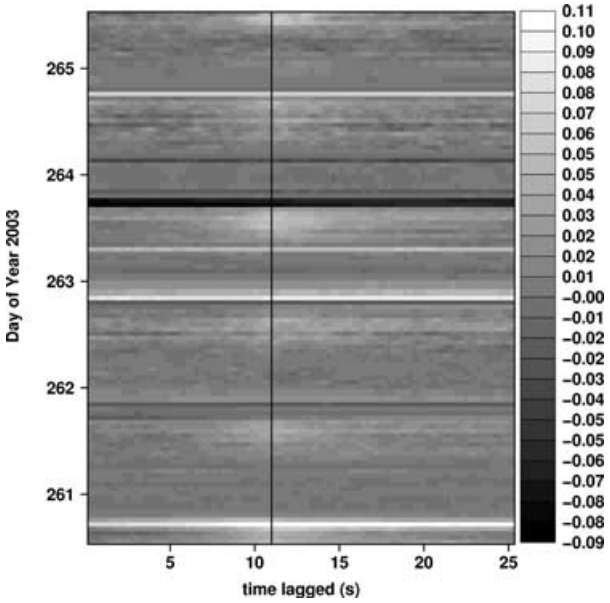

Fig. 3. Methanol fluxes plotted in time – lag time space. The diurnal flux cycle can be clearly identified and its maximum was labelled by the solid vertical line.

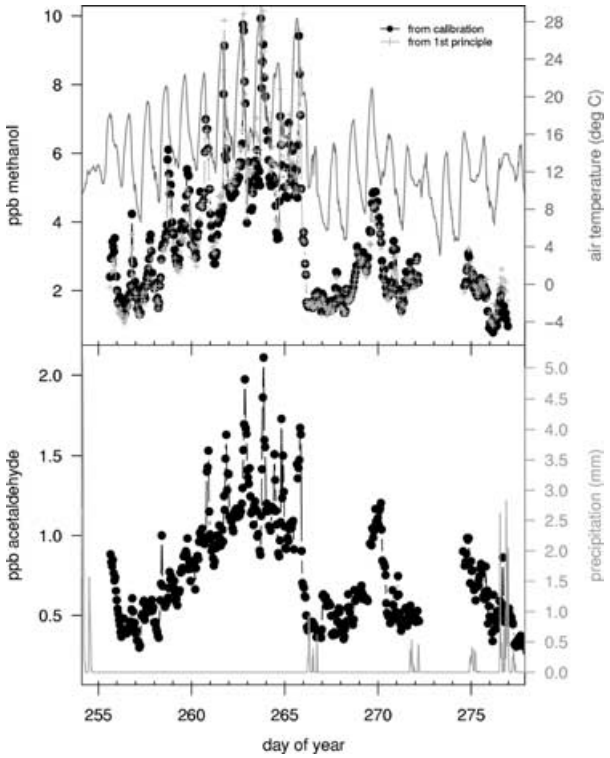

Fig. 4. Methanol and acetaldehyde mixing ratios during the 2003 field measurements, along with meteorological parameters. Methanol mixing ratio is split into calibrated data (filled black circles) and data calculated from first principles (grey pluses) showing excellent agreement. Obvious drift after day 275 make these data suspicious and they were not further analysed (see text).

data collection ceased due to cleaning/replacement of the PTR-MS ion source, freezing of the data collection computer or other hardware, or periods where parent ion signal or background were obviously erratic (often occurring just prior to normal replacement of the ion source for cleaning). Background corrections for methanol appear to be in error starting sometime after day 273 in 2003 (Fig. 2). Methanol data after day 276 drifted monotonously towards lower mixing ratios. For all measurements prior to day ∼276, methanol mixing ratios calculated based on standard gas addition and mixing ratios calculated from first principles compare well (Fig. 4). Although measurements were made before and after the range presented here, they have been omitted from discussion for this work.

For the time period presented, methanol mixing ratios ranged between 1 and 10 ppb, and acetaldehyde mixing ratios ranged from 0.3 to 2.1 ppbv, both comparing well with previously published levels in non-urban areas (Goldan et al., 1995, 2004; Riemer et al., 1998; Schade and Goldstein, 2001; Klouda et al., 2002; de Gouw et al., 2003b). Acetaldehyde mixing ratios correlated well with methanol mixing ratios with a linear fit r^2 value of 0.77. As apparent from Fig. 4, both methanol and acetaldehyde mixing ratios tracked ambient temperatures, which have previously been identified as a major driver of their emissions. A frontal passage with precipitation on day 266, connected to a typical Icelandic low pressure system and evident from sharp temperature and humidity gradients, lead to a change in air mass and to a rapid decrease of methanol and acetaldehyde mixing ratios. Back trajectories (HYSPLIT 4) indicated a regional, boundary layer origin prior to passage and a free tropospheric North Sea/North Atlantic origin after the frontal passage, as expected. Slight local anthropogenic influences on the measured mixing ratios from the city of Braunschweig located principally in the *SE* of the site were apparent when comparing wind roses of air temperature and methanol or acetaldehyde mixing ratio to each other. Figure 5 shows that temperatures and wind speeds were generally highest under northwesterly and northeasterly conditions, while mixing ratios maximized under low winds out of southern wind directions. Prior to the frontal passage, highest mixing ratios were generally observed at the onset of the stable nighttime boundary layer when wind speeds are lowest and continuing surface emissions accumulate in a shallower surface layer. This was confirmed when comparing the wind and OVOC data with onsite measurements of ozone for the same period, showing sharp declines in ozone mixing ratio due to titration by NO emissions at those same times. However, as no anthropogenic tracers were measured simultaneously, no definite conclusions about anthropogenic OVOC sources can be made.

Both methanol and acetaldehyde fluxes were available for a time period of rapid growth of the ryegrass in September. Figure 6 shows all methanol fluxes and incoming solar irradiance along with an estimated leaf area index (LAI) computed from a measured pre-harvest LAI of ∼ 5 (R. Manderscheid, FAL, personal communication 2005) and a standard logistic growth curve

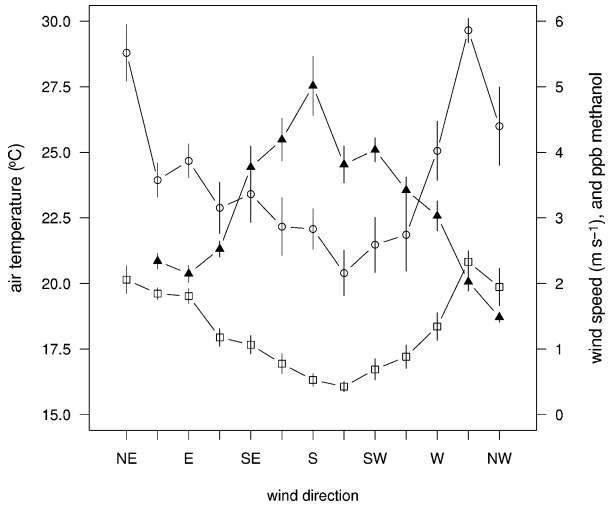

Fig. 5. Wind directional dependences of temperature (open circles), wind speed (open squares), and methanol mixing ratio (solid triangles) before day 273. Vertical bars are standard errors and indicate variability.

function extended out beyond our presented measurements past the time of harvest. Diurnally fluctuating methanol fluxes were observed prior to the frontal passage on mostly cloud-free days, while significantly lower and more erratic fluxes were observed during the subsequent colder period. We split the data into these two periods and show hourly binned OVOC fluxes in Fig. 7. For the acetaldehyde fluxes, no consistent diurnal cycle was found. Therefore, we conclude that acetaldehyde was neither emitted from the ryegrass, nor deposited to its surfaces or the soil surface in significant amounts. However, using the data set up until day 273, the period with highest confidence in the flux data, we calculated a median flux of -0.4 μg C m^{-2} h^{-1} with an interquartile range of -2.7 to 1.7 μg C m^{-2} h^{-1}. The median and lower quartile values translate into deposition velocities of 0.02–0.1 cm s^{-1}, lower than extrapolated from gradient measurements inside a tropical rain forest (Karl et al., 2004) and leaf level measurements on tropical plant species (Rottenberger et al., 2004, 2005). Similar to these previous studies though, acetaldehyde fluxes correlated weakly, but statistically significantly with its mixing ratio ($r^2 = 0.03$, $p = 0.002$, compensation point $= 0.6 \pm 0.7$ ppb). We conclude that there was likely a very slow net acetaldehyde deposition to the grass and soil surfaces.

In contrast, methanol fluxes were positive and moderately high during the warm period, and much smaller but significantly different from zero at daytime during the colder period (total range -0.08 to 0.12 mg C m^{-2} h^{-1}). In Fig. 8, all methanol flux data before day 277, acquired during periods of sufficient turbulence, and normalized to the estimated LAI were plotted against sonic virtual temperature as an indirect measure of leaf temperature. Similar to previous work (Schade and Goldstein, 2001; Karl et al., 2003), an exponential response to temperature was found with a β-factor of 0.15. As this response was calculated from a dataset under a wide range of ambient conditions, it can be considered representative. However, the calculation assumes that the leaf area specific methanol emissions are constant throughout leaf growth, contrary to previous findings that the leaf area specific methanol emissions were higher during the intensive growth stages of the investigated plant species (MacDonald and Fall, 1993; Nemecek-Marshall et al., 1995; Karl et al., 2003). To test the hypothesis that this is a physiological feature related to the origin of methanol as a by-product of pectin demethylation common to all plant species (Galbally and Kirstine, 2002),

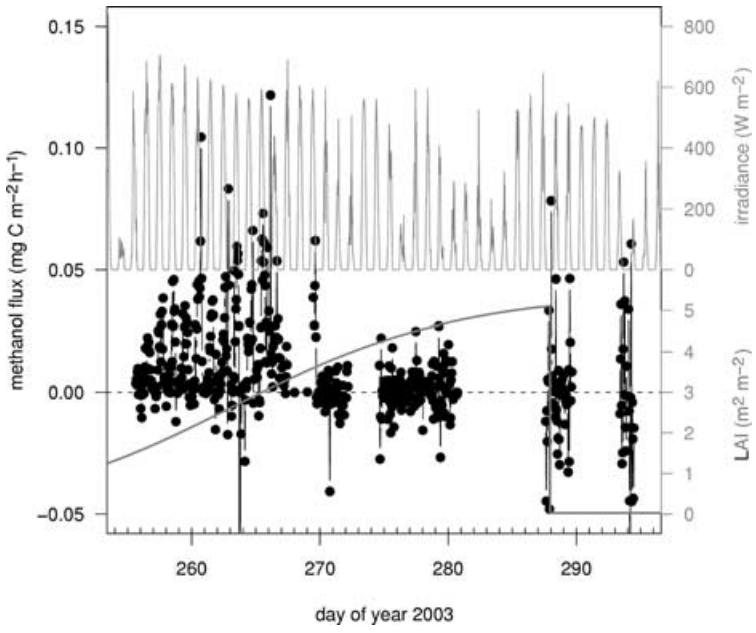

Fig. 6. Methanol fluxes, incoming solar irradiance, and estimated grass LAI during the complete measurement period.

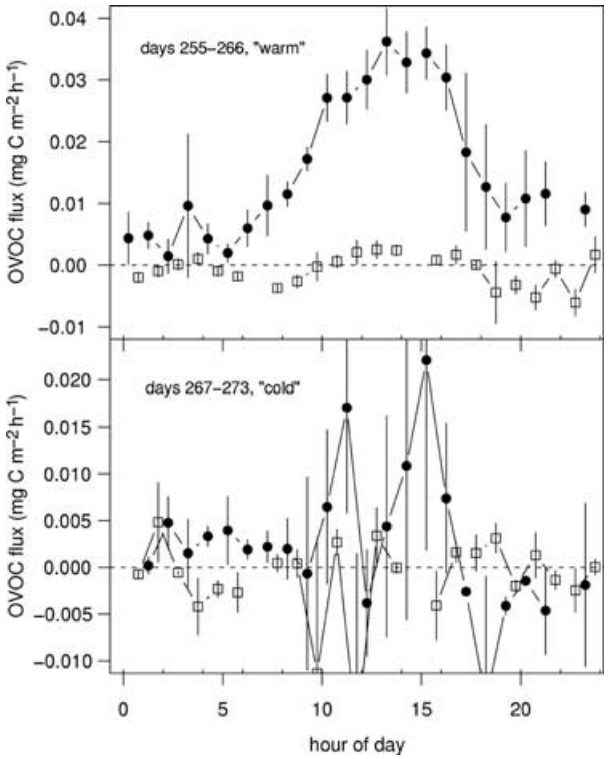

Fig. 7. Hourly binned methanol (filled circles) and acetaldehyde (open squares) fluxes with standard errors for two distinctly different meteorological periods named 'warm' and 'cold'. Note the difference in scale.

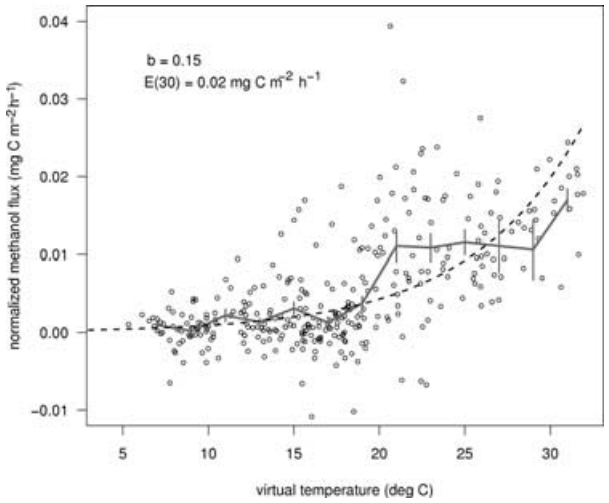

Fig. 8. Temperature-response of methanol emissions. Data (for a local $u*$ threshold of 0.05 m s^{-1}) in circles, 2 °C binned data with standard errors as solid grey line, and se-weighted response function according to $E = E_{30} \times \exp(\beta \times T_v)$ as dashed black line.

we further normalized the grass emissions by its temperature-modelled emissions. In Fig. 9, the ratio of measured to modelled emissions along with a local, polynomial regression model spanning ∼1 week is shown. The regression fit has a mean (median)

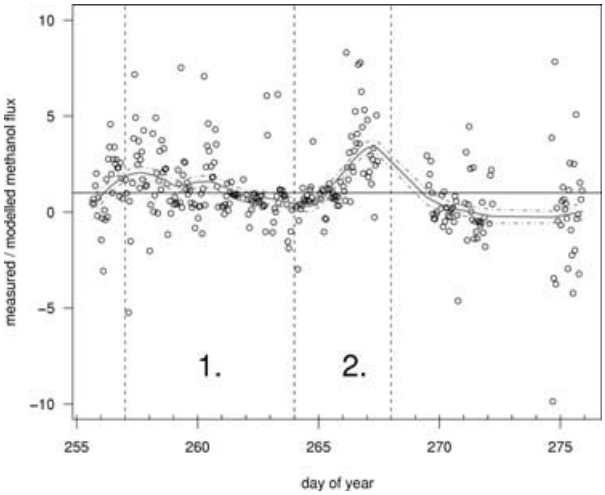

Fig. 9. LAI- and T-normalized methanol fluxes as a function of time. Solid grey line is a local regression model with estimated standard errors (dash–dotted lines). The horizontal black line marks the mean (=1.08), the unbiased response of a model sufficiently describing the data. The vertical dashed lines mark periods 1 and 2 described in the text.

of 1.08 (0.96) with a *SD* of 0.91, and there is little indication for a model bias. While this would seem at first to reject the hypothesis, there are several characteristics in the data that may allow for a different interpretation. First, during the initial 'warm' week a smaller variability is connected to a clear downward trend (Fig. 9, period 1), and second, a sharp increase of measured over modelled emissions (Fig. 9, period 2) is recorded right after the frontal passage rain (5.2 mm). The first period is assumed to be the one with the highest relative LAI increase per time, doubling the grass' biomass within a week (Fig. 6). The second period's rain may have (i) provided additional soil moisture to alleviate any plant water stress, likely also leading to additional growth not accounted for by our crude LAI estimate and/or (ii) triggered temporary methanol emissions from the dry topsoil (Warneke et al., 1999; Schade and Goldstein, 2001; Schade and Custer, 2004). While late season water stress occurred as a result of much lower seasonal soil moisture as a result of the dry and hot summer of 2003 (Löpmeier, 2004), a dry topsoil was certainly promoted by high irradiance, high temperatures, and the still rather open grass canopy during this period. Further support for the assumption of higher specific methanol emissions during the initial growth phase of the grass is provided by the consistently lower measured than modelled methanol emissions along with comparatively small LAI changes after this rain-triggered, temporary increase. It appears therefore that the expected decrease of methanol emissions with growth progression was, in our case, only masked by a rain event.

Complicating the above analysis is the fact that the micrometeorological measurements yield a net flux from the surface, including both soil and plant exchanges. Jacob et al. (2005)

assumed that a global average methanol deposition velocity of 0.2 cm s^{-1} is necessary to close its atmospheric budget. However, evidence for both higher deposition velocities (Karl et al., 2004) and soil emissions (Schade and Custer, 2004, and references therein) exist. Consistently positive fluxes measured during the warm period nights (Fig. 7) along with the assumption that plant methanol is only emitted through open stomata, suggest that, similar to our previous report (Schade and Custer, 2004), a dry topsoil may have acted as a source of methanol. During the subsequent cold period, nighttime fluxes were essentially zero (Fig. 7) suggesting that the wetter soil was not an efficient sink for methanol at this time either. Hence, we conclude that the observed fluxes were a combination of a small soil source and a larger plant source, the former partially obscuring the study of a trend in the specific methanol emissions from the grass.

This conclusion does not exclude the possibility that the soil acts as a net sink for methanol at higher soil moistures and on a long-term basis. Although omitted from this work, mean flux from after the grass was harvested and removed from the plot suggested a deposition velocity of ∼0.1 cm s^{-1} assuming an abundance of 2 ppb methanol. Although tenuous in light of instrumental instabilities after day 277, this result prompted a more detailed soil trace gas exchange study using a flux chamber over the same field in 2004, which will be reported elsewhere.

4. Conclusions

We provide the first observations of methanol and acetaldehyde fluxes above a grass species using the eddy covariance technique. We previously used PTR-MS in conjunction with sonic anemometer data successfully to measure OVOC fluxes at this site (Schade and Custer, 2004), and have provided here a more detailed description of the necessary data handling procedures to yield useful flux information. While significant methanol emissions were recorded, very little acetaldehyde exchange was detected. We estimated from our flux and mixing ratio data that acetaldehyde may on average have been deposited to the surface at a deposition velocity of 0.05 cm s^{-1} with an uncertainty of at least a factor of two. This level is at the lower end of published results from measurements on deciduous plant species (Rottenberger et al., 2005, and references therein) and may characterize grasses and soil as rather inefficient acetaldehyde adsorption surfaces.

The observed methanol emissions (∼0–0.03 mg C m^{-2} h^{-1} interquartile range) were also smaller compared to previous studies in forested environments and this may be interpreted as a confirmation of the hypothesis forwarded by Galbally and Kirstine (2002) that grasses should emit several times less methanol as compared to, for instance, tree species because they have much less pectin in their cell walls. Our results compare favourably with grassland measurements of Fukui and Doskey (1998) and Kirstine et al. (1998) with the exception that the latter found acetaldehyde emissions of a similar magnitude to methanol emissions, while the former also found acetaldehyde emissions to be ten times lower than methanol emissions. Methanol emissions from these works are within a factor of two of our results taking temperature into account, providing further evidence that methanol emissions of this magnitude (i.e. $E_{30} \approx 0.1$ mg C m^{-2} h^{-1}) are a common feature of all grasslands. While the two previous works on grasses and the measurements over forested environments (Schade and Goldstein, 2001; Karl et al., 2003) found methanol emission temperature response factors smaller than 0.12, our results indicate a higher value. The discrepancy may be reconciled based on the fact that all high temperature observations in this work were made during the grass' rapid growth phase. Reducing those emissions by a factor of 2 to account for this effect, reduced the calculated β-factor to 0.12 ± 0.03 bringing it into the range of previous estimates. Using this basic exponential temperature response in the simple global model outlined by Schade and Crutzen (1999), assuming β to range from 0.05 to 0.15 and E_{30} from 0.05 to 0.2 mg C m^{-2} h^{-1}, we calculated a global annual methanol emission from grasslands of 5 ± 4 Tg C yr^{-1}, which compares satisfactorily with earlier estimates (Galbally and Kirstine, 2002; Jacob et al., 2005). This independent estimate based on our field data confirms that grassland ecosystems exhibit lower methanol emissions as compared to non-grass dominated ecosystems. Grasslands may only contribute approximately 10% to global green plant methanol emissions, and future methanol flux measurements should concentrate on the presumed pectin source and whether control of emissions by plant stomata strongly influences measured fluxes in various non-grass ecosystems.

5. Acknowledgments

This research was made possible by the Deutsche Forschungsgemeinschaft (DFG) under Emmy-Noether grant SCHA922/2–1. The authors thank the employees of the FAL-Agraroekologie section, particularly Dr. Andreas Pacholski, for their collaboration in and tireless support of this project.

References

Andreae, M. O. and Crutzen, P. J. 1997. Atmospheric aerosols: biogeochemical sources and role in atmospheric chemistry. *Science* **276**(5315), 1052–1058.

Arey, J., Winer, A. M., Atkinson, R., Aschmann, S. M., Long, W. D. and co-authors. 1991. The emission Of (Z)-3-hexen-1-Ol, (Z)-3-hexenylacetate and other oxygenated hydrocarbons from agricultural plant-species. *Atmos. Environ.* **25**(5–6), 1063–1075.

Baker, B., Guenther, A., Greenberg, J. and Fall, R. 2001. Canopy level fluxes of 2-methyl-3-buten-2-ol, acetone, and methanol by a

portable relaxed eddy accumulation system. *Environ. Sci. Technol.* **35**(9), 1701–1708.

Chameides, W. L., Lindsay, R. W., Richardson, J. and Kiang, C. S. 1988. The role of biogenic hydrocarbons in urban photochemical smog—Atlanta as a case-study. *Science* **241**(4872), 1473–1475.

Chameides, W. L., Fehsenfeld, F., Rodgers, M. O., Cardelino, C., Martinez, J. and co-authors. 1992. Ozone precursor relationships in the ambient atmosphere. *J. Geophys. Res.* **97**(D5), 6037–6055.

Custer, T. G., Kato, S., Fall, R. and Bierbaum, V. A. 2003. Negative-ion CIMS: analysis of volatile leaf wound compounds including HCN. *Int. J. Mass Spectrom.* **223**(1–3), 427–446.

de Gouw, J. A., Howard, C. J., Custer, T. G., Baker, B. M. and Fall, R. 2000. Proton-transfer chemical-ionization mass spectrometry allows real-time analysis of volatile organic compounds released from cutting and drying of crops. *Environ. Sci. Technol.* **34**(12), 2640–2648.

de Gouw, J. A., Howard, C. J., Custer, T. G. and Fall, R. 1999. Emissions of volatile organic compounds from cut grass and clover are enhanced during the drying process. *Geophys. Res. Lett.* **26**(7), 811–814.

de Gouw, J., Warneke, C., Karl, T., Eerdekens, G., van der Veen, C. and co-authors. 2003a. Sensitivity and specificity of atmospheric trace gas detection by proton-transfer-reaction mass spectrometry. *Int. J. Mass Spectrom.* **223**(1–3), 365–382.

de Gouw, J. A., Goldan, P. D., Warneke, C., Kuster, W. C., Roberts, J. M. and co-authors. 2003b. Validation of proton transfer reaction-mass spectrometry (PTR-MS) measurements of gas-phase organic compounds in the atmosphere during the New England Air Quality Study (NEAQS) in 2002. *J. Geophys. Res.* **108**(D21), 4682, doi:10.1029/2003JD003863.

Fall, R. 2003. Abundant oxygenates in the atmosphere: a biochemical perspective. *Chem. Rev.* **103**(12), 4941–4951.

Fall, R. and Benson, A. A. 1996. Leaf methanol—the simplest natural product from plants. *Tr. Plant Sci.* **1**(9), 296–301.

Fall, R., Karl, T., Hansel, A., Jordan, A. and Lindinger, W. 1999. Volatile organic compounds emitted after leaf wounding: on-line analysis by proton-transfer-reaction mass spectrometry. *J. Geophys. Res.* **104**(D13), 15963–15974.

Fukui, Y. and Doskey, P. V. 1998. Air-surface exchange of nonmethane organic compounds at a grassland site: seasonal variations and stressed emissions. *J. Geophys. Res.* **103**(D11), 13153–13168.

Galbally, I. E. and Kirstine, W. 2002. The production of methanol by flowering plants and the global cycle of methanol. *J. Atmos. Chem.* **43**(3), 195–229.

Goldan, P. D., Kuster, W. C., Fehsenfeld, F. C. and Montzka, S. A. 1995. Hydrocarbon measurements in the southeastern United States: the Rural Oxidants in the Southern Environment (ROSE) program 1990. *J. Geophys. Res.* **100**(D12), 25945–25963.

Goldan, P. D., Kuster, W. C., Williams, E., Murphy, P. C., Fehsenfeld, F. C. and co-authors. 2004. Nonmethane hydrocarbon and oxy hydrocarbon measurements during the 2002 New England Air Quality Study. *J. Geophys. Res.* **109**(D21), D21309, doi:10.1029/2003JD004455.

Goode, J. G., Yokelson, R. J., Susott, R. A. and Ward, D. E. 1999. Trace gas emissions from laboratory biomass fires measured by open-path Fourier transform infrared spectroscopy: fires in grass and surface fuels. *J. Geophys. Res.* **104**(D17), 21237–21245.

Graus, M., Schnitzler, J. P., Hansel, A., Cojocariu, C., Rennenberg, H. and co-authors. 2004. Transient release of oxygenated volatile organic compounds during light-dark transitions in grey poplar leaves. *Plant Physiol.* **135**(4), 1967–1975.

Guenther, A., Hewitt, C. N., Erickson, D., Fall, R., Geron, C. and co-authors. 1995. A global-model of natural volatile organic-compound emissions. *J. Geophys. Res.* **100**(D5), 8873–8892.

Harley, P., Vasconcellos, P., Vierling, L., Pinheiro, C. C. D., Greenberg, J. and co-authors. 2004. Variation in potential for isoprene emissions among Neotropical forest sites. *Glob. Change Biol.* **10**(5), 630–650.

Heikes, B. G., Chang, W. N., Pilson, M. E. Q., Swift, E., Singh, H. B. and co-authors. 2002. Atmospheric methanol budget and ocean implication. *Global Biogeochem. Cycles* **16**(4), 1133, doi:10.1029/2002GB001895.

Hojstrup, J. 1993. A statistical-data screening-procedure. *Measur. Sci. Technol.* **4**(2), 153–157.

Holzinger, R., Warneke, C., Hansel, A., Jordan, A., Lindinger, W. and co-authors. 1999. Biomass burning as a source of formaldehyde, acetaldehyde, methanol, acetone, acetonitrile, and hydrogen cyanide. *Geophys. Res. Lett.* **26**(8), 1161–1164.

Jacob, D. J., Field, B. D., Li, Q. B., Blake, D. R., de Gouw, J. and co-authors. 2005. Global budget of methanol: constraints from atmospheric observations. *J. Geophys. Res.* **110**(D8), D08303, doi:10.1029/2004JD005172.

Kaimal, J. C. and Finnagan, J. J. 1994. *Atmospheric Boundary Layer Flows: Their Structure and Measurement*. Oxford University Press, New York, pp. 289.

Karl, T., Guenther, A., Jordan, A., Fall, R. and Lindinger, W. 2001a. Eddy covariance measurement of biogenic oxygenated VOC emissions from hay harvesting. *Atmos. Environ.* **35**(3), 491–495.

Karl, T., Guenther, A., Lindinger, C., Jordan, A., Fall, R. and co-authors. 2001b. Eddy covariance measurements of oxygenated volatile organic compound fluxes from crop harvesting using a redesigned proton-transfer-reaction mass spectrometer. *J. Geophys. Res.* **106**(D20), 24157–24167.

Karl, T., Guenther, A., Spirig, C., Hansel, A. and Fall, R. 2003. Seasonal variation of biogenic VOC emissions above a mixed hardwood forest in northern Michigan. *Geophys. Res. Lett.* **30**(23), 2186, doi:10.1029/2003GL018432.

Karl, T., Harley, P., Guenther, A., Rasmussen, R., Baker, B. and co-authors. 2005a. The bi-directional exchange of oxygenated VOCs between a loblolly pine (*Pinus taeda*) plantation and the atmosphere. *Atmos. Chem. Phys.* **5**, 3015–3031.

Karl, T., Harren, F., Warneke, C., de Gouw, J., Grayless, C. and co-authors. 2005b. Senescing grass crops as regional sources of reactive volatile organic compounds. *J. Geophys. Res.* **110**(D15).

Karl, T., Potosnak, M., Guenther, A., Clark, D., Walker, J. and co-authors. 2004. Exchange processes of volatile organic compounds above a tropical rain forest: implications for modeling tropospheric chemistry above dense vegetation. *J. Geophys. Res.* **109**(D18), D18306, doi:10.1029/2004JD004738.

Karl, T. G., Spirig, C., Rinne, J., Stroud, C., Prevost, P. and co-authors. 2002. Virtual disjunct eddy covariance measurements of organic compound fluxes from a subalpine forest using proton transfer reaction mass spectrometry. *Atmos. Chem. Phys.* **2**, 279–291.

Kesselmeier, J. 2001. Exchange of short-chain oxygenated volatile organic compounds (VOCs) between plants and the atmosphere: a

compilation of field and laboratory studies. *J. Atmos. Chem.* **39**(3), 219–233.

Kesselmeier, J., Bode, K., Hofmann, U., Muller, H., Schafer, L. and co-authors. 1997. Emission of short chained organic acids, aldehydes and monoterpenes from *Quercus ilex* L. and *Pinus pinea* L. in relation to physiological activities, carbon budget and emission algorithms. *Atmos. Environ.* **31**, 119–133.

Kesselmeier, J. and Staudt, M. 1999. Biogenic volatile organic compounds (VOC): an overview on emission, physiology and ecology. *J. Atmos. Chem.* **33**(1), 23–88.

Kirstine, W., Galbally, I., Ye, Y. R. and Hooper, M. 1998. Emissions of volatile organic compounds (primarily oxygenated species) from pasture. *J. Geophys. Res.* **103**(D9), 10605–10619.

Klouda, G. A., Lewis, C. W., Stiles, D. C., Marolf, J. L., Ellenson, W. D. and co-authors. 2002. Biogenic contributions to atmospheric volatile organic compounds in Azusa, California. *J. Geophys. Res.* **107**(D7–8), doi:10.1029/2001JD000758.

König, G., Brunda, M., Puxbaum, H., Hewitt, C. N., Duckham, S. C. and co-authors. 1995. Relative contribution of oxygenated hydrocarbons to the total biogenic VOC emissions of selected mid-European agricultural and natural plant-species. *Atmos. Environ.* **29**(8), 861–874.

Kreuzwieser, J., Kuhnemann, F., Martis, A., Rennenberg, H. and Urban, W. 2000. Diurnal pattern of acetaldehyde emission by flooded poplar trees. *Physiol. Plant.* **108**(1), 79–86.

Kreuzwieser, J., Scheerer, U. and Rennenberg, H. 1999. Metabolic origin of acetaldehyde emitted by poplar (*Populus tremula* × *P. alba*) trees. *J. Exp. Bot.* **50**(335), 757–765.

Löpmeier, F. J. 2004. Das Trockenjahr 2003 aus agrarmeteorologischer Sicht. In: *Klimastatusbericht 2003*, Deutscher Wetterdienst, Offenbach, Germany, pp. 190.

Macdonald, R. C. and Fall, R. 1993. Detection of substantial emissions of methanol from plants to the atmosphere. *Atmos. Environ.* **27**(11), 1709–1713.

McKeen, S. A., Hsie, E. Y., Trainer, M., Tallamraju, R. and Liu, S. C. 1991. A regional model study of the ozone budget in the eastern United-States. *J. Geophys. Res.* **96**(D6), 10809–10845.

Moncrieff, J. B., Massheder, J. M., de Bruin, H., Elbers, J., Friborg, T. and co-authors. 1997. A system to measure surface fluxes of momentum, sensible heat, water vapour and carbon dioxide. *J. Hydrol.* **189**(1–4), 589–611.

Nemecek-Marshall, M., Macdonald, R. C., Franzen, F. J., Wojciechowski, C. L. and Fall, R. 1995. Methanol emission from leaves – enzymatic detection of gas-phase methanol and relation of methanol fluxes to stomatal conductance and leaf development. *Plant Physiol.* **108**(4), 1359–1368.

Northway, M. J., de Gouw, J. A., Fahey, D. W., Gao, R. S., Warneke, C. and co-authors. 2004. Evaluation of the role of heterogeneous oxidation of alkenes in the detection of atmospheric acetaldehyde. *Atmos. Environ.* **38**(35), 6017–6028.

R Development Core Team. 2005. R: a language and environment for statistical computing. In: *R Foundation for Statistical Computing*, Vienna, Austria.

Riemer, D., Pos, W., Milne, P., Farmer, C., Zika, R. and co-authors. 1998. Observations of nonmethane hydrocarbons and oxygenated volatile organic compounds at a rural site in the southeastern United States. *J. Geophys. Res.* **103**(D21), 28111–28128.

Rinnan, R., Rinnan, A., Holopainen, T., Holopainen, J. K. and Pasanen, P. 2005. Emission of non-methane volatile organic compounds (VOCs) from boreal peatland microcosms – effects of ozone exposure. *Atmos. Environ.* **39**(5), 921–930.

Rottenberger, S., Kuhn, U., Wolf, A., Schebeske, G., Oliva, S. T. and co-authors. 2004. Exchange of short-chain aldehydes between Amazonian vegetation and the atmosphere. *Ecol. Appl.* **14**(4), S247–S262.

Rottenberger, S., Kuhn, U., Wolf, A., Schebeske, G., Oliva, S. T. and co-authors. 2005. Formaldehyde and acetaldehyde exchange during leaf development of the Amazonian deciduous tree species *Hymenaea courbaril*. *Atmos. Environ.* **39**(12), 2275–2279.

Schade, G. W. and Crutzen, P. J. 1999. CO emissions from degrading plant matter (II). Estimate of a global source strength. *Tellus* **51B**(5), 909–918.

Schade, G. W. and Custer, T. G. 2004. OVOC emissions from agricultural soil in northern Germany during the 2003 European heat wave. *Atmos. Environ.* **38**(36), 6105–6114.

Schade, G. W. and Goldstein, A. H. 2001. Fluxes of oxygenated volatile organic compounds from a *Ponderosa pine* plantation. *J. Geophys.l Res.* **106**(D3), 3111–3123.

Schnitzler, J. P., Bauknecht, N., Bruggemann, N., Einig, W., Forkel, R. and co-authors. 2002. Emission of biogenic volatile organic compounds: an overview of field, laboratory and modelling studies performed during the 'Tropospheric Research Program' (TFS) 1997–2000. *J. Atmos. Chem.* **42**(1), 159–177.

Sharkey, T. D. 1996. Emission of low molecular mass hydrocarbons from plants. *Tr. Plant Sci.* **1**(3), 78–82.

Sillman, S. 1999. The relation between ozone, NO_x and hydrocarbons in urban and polluted rural environments. *Atmos. Environ.* **33**(12), 1821–1845.

Singh, H., Chen, Y., Tabazadeh, A., Fukui, Y., Bey, I. and co-authors. 2000. Distribution and fate of selected oxygenated organic species in the troposphere and lower stratosphere over the Atlantic. *J. Geophys. Res.* **105**(D3), 3795–3805.

Singh, H. B., Salas, L. J., Chatfield, R. B., Czech, E., Fried, A. and co-authors. 2004. Analysis of the atmospheric distribution, sources, and sinks of oxygenated volatile organic chemicals based on measurements over the Pacific during TRACE-P. *J. Geophys. Res.* **109**(D15), D15S07, doi:10.1029/2003JD003883.

Steinbacher, A., Dommen, J., Ammann, C., Spirig, C., Neftel, A. and co-authors. 2004. Performance characteristics of a proton-transfer-reaction mass spectrometer (PTR-MS) derived from laboratory and field measurements. *Int. J. Mass Spectrom.* **239**(2–3), 117–128.

Tie, X., Guenther, A. and Holland, E. 2004. Biogenic methanol and its impacts on tropospheric oxidants. *Geophys. Res. Lett.* **30**(17), 1881, doi:10.1029/2003GL017167.

Warneke, C., De Gouw, J. A., Kuster, W. C., Goldan, P. D. and Fall, R. 2003. Validation of atmospheric VOC measurements by proton-transfer-reaction mass spectrometry using a gas-chromatographic preseparation method. *Environ. Sci. Technol.* **37**(11), 2494–2501.

Warneke, C., Karl, T., Judmaier, H., Hansel, A., Jordan, A. and co-authors. 1999. Acetone, methanol, and other partially oxidized volatile organic emissions from dead plant matter by abiological processes: significance for atmospheric HOx chemistry. *Global Biogeochem. Cycles* **13**(1), 9–17.

Warneke, C., Luxembourg, S. L., de Gouw, J. A., Rinne, H. J. I., Guenther, A. B. and co-authors. 2002. Disjunct eddy covariance measurements of oxygenated volatile organic compounds fluxes from an

alfalfa field before and after cutting. *J. Geophys. Res.* **107**(D7–8), doi:10.1029/2001JD000594.

Winer, A. M., Arey, J., Atkinson, R., Aschmann, S. M., Long, W. D. and co-authors. 1992. Emission rates of organics from vegetation in California Central Valley. *Atmos. Environ.* **26**(14), 2647–2659.

Yokelson, R. J., Goode, J. G., Ward, D. E., Susott, R. A., Babbitt, R. E. and co-authors. 1999. Emissions of formaldehyde, acetic acid, methanol, and other trace gases from biomass fires in North Carolina measured by airborne Fourier transform infrared spectroscopy. *J. Geophys. Res.* **104**(D23), 30109–30125.